

Ultra-Wideband Air-Filled SIW Cavity-Backed Slot Antenna with Multipolarization Reconfiguration

Kamil Yavuz Kapusuz, Sam Lemey, Hendrik Rogier

Department of Information Technology, IDLab/Electromagnetics Group, imec-Ghent University, Belgium

KamilYavuz.Kapusuz@UGent.be, Sam.Lemey@UGent.be, Hendrik.Rogier@UGent.be

Abstract—Air-filled substrate integrated waveguide (AFSIW) cavity-backed slot antenna topologies are promising candidates to address the specific design challenges posed by the Internet of Things (IoT). In this contribution, we demonstrate a new single-feed ultrawideband cavity-backed slot antenna with multipolarization reconfiguration by leveraging four quartets of PIN diodes in substrate-independent AFSIW technology for operation in the [5.15-5.85] GHz frequency band. To achieve ultra-wideband performance, two concentric annular slots are created on the top of the circular cavity. By electrically shorting these annular slots at well-defined positions by the aforementioned PIN diodes, dynamic polarization reconfiguration is achieved by switching their DC bias current. Moreover, a systematic investigation of the different loss contributions and power consumption is performed. A physical explanation of the different effects is also provided. Finally, a fabricated prototype exhibits a measured impedance bandwidth of 1.6 GHz (or 29%), a total efficiency higher than 74%, and a gain higher than 5.2 dBi for all four states in free-space conditions.

Index Terms—Air-filled substrate integrated waveguide (AFSIW), cavity-backed slot antenna, multipolarization reconfigurable, PIN diodes, reconfigurable antennas, substrate integrated waveguide (SIW).





I. INTRODUCTION

With the significant advancement in the Internet of Things (IoT), explosive growth in connected things, devices, and machines is foreseen in the near future. As a result, global data traffic is expected to skyrocket [1], [2]. Moreover, these trends fuel the need for massive data rate enhancement in all branches of communication infrastructures. Likewise, wireless data rates are trying to keep up with ever-increasing data rates needed by future wireless applications. In this evolution, compact ultra-wideband polarization-agile antenna systems play an essential role [3]. Yet, while these advanced antenna systems provide many opportunities, they also bring many challenges and requirements [4].

The signal quality offered by different receive antennas for incident waves with various polarizations is compared in Table I. Circular polarizations (CP) and two orthogonal linear polarization (LP) antennas receive any linearly polarized wave with a maximum efficiency of 50% [5]. Moreover, there is a possibility of complete polarization mismatch when receiving an arbitrary CP wave with a CP antenna. In contrast, the polarization efficiency can be significantly improved by switching a reconfigurable antenna between four linear polarizations [6].

To fulfill the required design challenges in terms of optimum performance and cost, various multilinear polarization-

TABLE I
SIGNAL QUALITY OBTAINED BY RECEIVE ANTENNAS FOR INCIDENT WAVES WITH VARIOUS POLARIZATIONS

	LHCP	RHCP	Dual LP	Multi LP
				
HP	50% Loss	50% Loss	50% Loss	0% Loss
VP	50% Loss	50% Loss	50% Loss	0% Loss
RHCP	100% Loss	0% Loss	50% Loss	50% Loss
LHCP	0% Loss	100% Loss	50% Loss	50% Loss

LP: Linear polarization, CP: Circular polarization,
HP: Horizontal polarization, VP: Vertical polarization,
RHCP: Right-handed CP, LHCP: Left-handed CP.

reconfigurable antennas have been developed, mainly focusing on reconfigurable feeding networks [7], [8] and radiating elements [9]–[15]. Yet, exploiting reconfigurable feeding networks in the design typically suffers from significant losses in the feed network, large size, and complexity proportional to the number of switching states. Moreover, utmost care is needed to prevent electromagnetic interference (EMI) issues due to unwanted radiation. Hence, a reconfigurable radiating element can be an alternative to reduce the feed network loss, system size, and complexity.

In this contribution, we present a multipolarization-reconfigurable air-filled substrate integrated waveguide (AFSIW) cavity-backed slot antenna, offering high performance for low-cost IoT devices. By incorporating sixteen PIN diodes on two concentric annular slots, the antenna is able to alter its polarization among four different states, while providing ultra-wideband antenna performance. Dynamic switching between four linear polarization states is achieved by an external bias tee and an innovative biasing network that exploits the AFSIW sidewalls to route the required DC bias currents to the PIN diodes in the antenna cavity. Owing to the intrinsic symmetry of the structure, the cross-polarization is additionally reduced for four polarization states. In contrast to [16], [17], where the direct and invisible integration of a dual-linear polarization-reconfigurable AFSIW cavity-backed slot antenna inside the worktop of a desk is presented, the design in this work features dynamic switching between four linear polarization states. In addition to our work in [18], where an AFSIW cavity-backed slot antenna with multipolarization reconfiguration is presented, we now investigate the loss and power consumption of the dynamic switching between four linear polarization states in more detail.

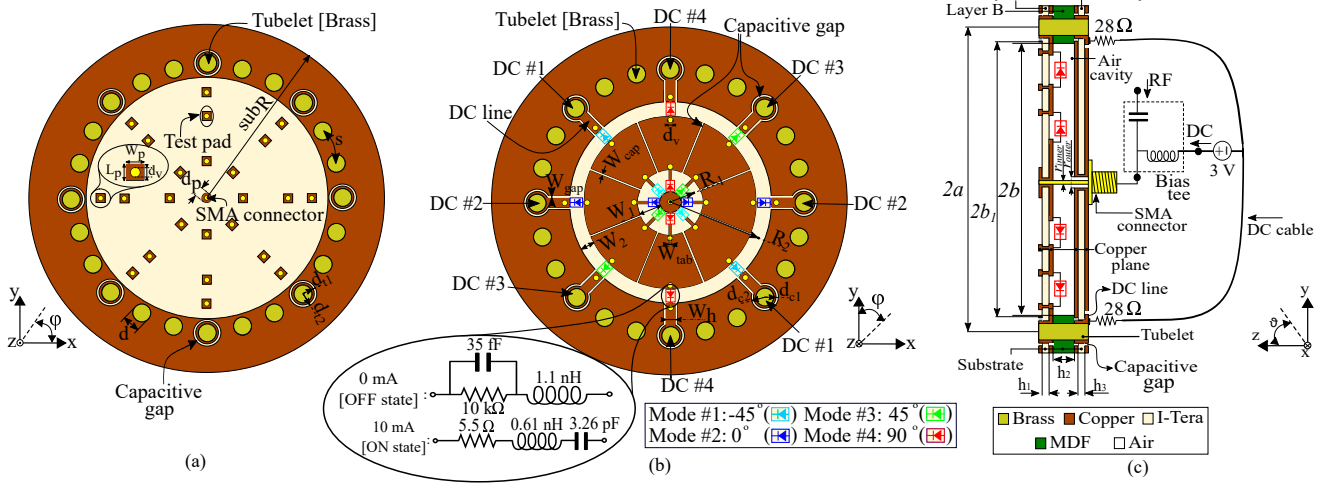


Fig. 1. Multipolarization-reconfigurable AFSIW cavity-backed slot antenna. (a) Front side of Layer A. (b) Back side of Layer A. (c) Cross section view. Optimized dimensions: Optimized dimensions: $sub_R = 55.0$ mm, $a = 30.5$ mm, $b = b_1 = 27.9$ mm, $R_1 = 4.55$ mm, $W_1 = 5.1$ mm, $R_2 = 22.3$ mm, $W_2 = 3.5$ mm, $W_{tab} = 0.2$ mm, $W_{cap} = 0.1$ mm, $W_{gap} = 0.15$ mm, $W_p = 1.5$ mm, $W_h = 1.8$ mm, $L_p = 1.5$ mm, $d_v = 1.0$ mm, $h_1 = h_3 = 0.25$ mm, $h_2 = 4.0$ mm, $d = 4.0$ mm, $d_p = 2.5$ mm, $d_{c1} = d_{t1} = 3.35$ mm, $d_{c2} = d_{t2} = 3.5$ mm, $s = 15^\circ$, $r_{inner} = 1.3$ mm, $r_{outer} = 4.3$ mm. Substrate parameters at 5.5 GHz: Layers A and C are implemented in I-Tera ($\epsilon_r = 3.43$, $\tan\delta = 0.014$), Layer B is implemented in medium-density fibreboard (MDF) material ($\epsilon_r = 2.21$, $\tan\delta = 0.06$).

II. MULTIPOLARIZATION RECONFIGURABLE ANTENNA

The proposed reconfigurable antenna is based on the AFSIW cavity-backed slot antenna shown in Fig. 1, whose basic topology was initially proposed in [16] in a non-reconfigurable setup, which consists of a circular AFSIW cavity and two concentric annular slots. As shown in [17], splitting these rings in two by shorting tabs provides control of the polarization. Meanwhile, the cavity-backed slot antenna is implemented by exploiting the substrate-independent AFSIW technology proposed in [19], [20].

The developed ultra-wideband AFSIW multipolarization reconfigurable antenna can be decomposed into three dielectric layers (Layer A, Layer B, Layer C) and four conductor layers. Layer A and Layer C implement the top and bottom conducting boundaries of the cavity [18]. They sandwich Layer B through an array of metallic vias, implemented by tubelets, which also tighten the complete layer stack. The design of the antenna is carried out by optimizing the cavity dimensions and annular slot sizes for the desired bandwidth, exploiting the design procedure described in [17]. First, the cavity radius a is calculated, ensuring monomodal wave propagation of the TM_{01} mode in the circular AFSIW section forming the backing cavity of the antenna. Second, resonant annular ring slots are designed in Layer A. Subsequently, two diametrically positioned shorting tabs are added to split the annular slot in two. In each half-ring radiating aperture, the $TM_{01, waveguide}$ mode propagating in the circular cross-section of the feeding cavity is converted into the $TE_{11, slot}$ even mode of that slot, producing a conical radiation pattern. Remark that the angular location of the shorting tabs on the slot defines the direction along which the electric field is linearly polarized.

To implement compact and cost-effective reconfiguration between four linear polarizations, the AFSIW antenna topol-

ogy, shown in Fig. 1, is adopted. Rather than fixing the polarization by the angular locations of the shorting tabs in Layer A, dynamic reconfiguration is achieved by replacing these short circuits by PIN diodes at carefully selected angular positions [see Fig. 1(b)]. Their DC bias currents are supplied at the antenna feed through an external bias tee and routed from the antenna's back to the front cavity plane via the AFSIW sidewalls. In this way, it is possible to route the DC bias current from the front side of the antenna to the backside. To dynamically and independently control each quartet of PIN diodes, capacitive gaps are created in Layers A and C [Fig. 1] to decouple the DC grounds of the diodes. By applying the positive polarity to the antenna feed line through an external bias tee [see Fig. 1(c)], while the other polarity is supplied to the DC#3 pins and not to the other DC biasing lines [see Fig. 4(d)], the green-colored diode quartet [see Fig. 1(b)] is brought in the ON state and the other diodes are switched OFF, yielding a -45° linear polarization. Similarly, by switching the polarity from DC#3 to other DC lines, the polarization state can switch between any of the four states. In the design, the current through each diode is set to 10 mA by adding a $28\ \Omega$ series resistor to each DC wire at the back of the antenna. A supply voltage of 3 V is provided through the external bias tee [see Fig. 1(c)]. This new simple bias network allows integrating all polarization control electronics inside the antenna cavity to protect them from environmental effects and provide straightforward integration of the antenna inside a common surface.

III. PERFORMANCE ANALYSIS

A. Loss Mechanism versus Antenna Efficiency

To characterize the loss mechanisms of the antenna, a detailed power analysis is conducted [21], [22]. The radiation

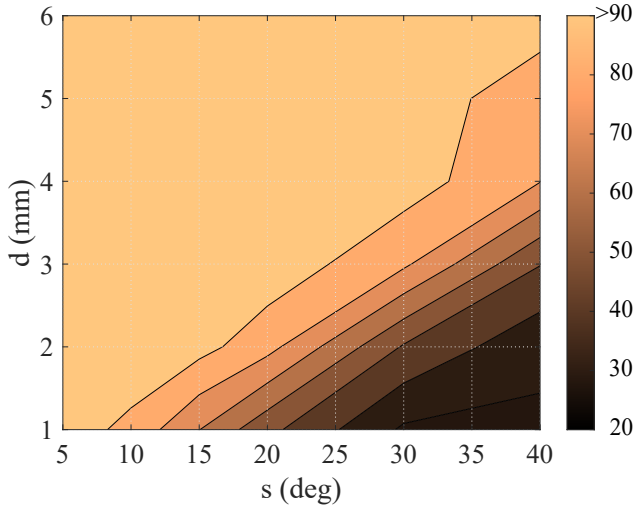


Fig. 2. Radiation efficiency (%) at 5.5 GHz versus the diameter of the tubelets (d) and angular spacing between the tubelets (s), implementing the AFSIW sidewall.

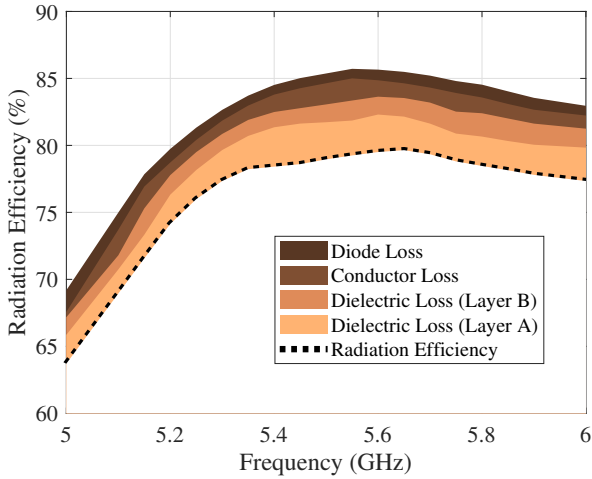


Fig. 3. Radiation efficiency (%) losses occurring in the antenna topology and its components.

and total antenna efficiencies are computed as a function of frequency.

Fig. 2 depicts the radiation efficiency at 5.5 GHz due to leakage losses, versus d and s [Fig. 1(a)] for the nonreconfigurable design presented in [16]. The radiation efficiency is small due to the large leakage losses when the metal vias are small and far apart, i.e., when the gaps between the vias are wide. In particular, the radiation efficiency is higher than 90% when the angular spacing s is about 10° for the smallest metal via diameter d .

Besides leakage losses due to leakage through the gaps between tubelets, dielectric losses due to the substrate material supporting the side walls and upper conducting layer, conductor losses in the metal, and diode loss will also be present in the antenna [Fig. 1]. The contributions of the different loss

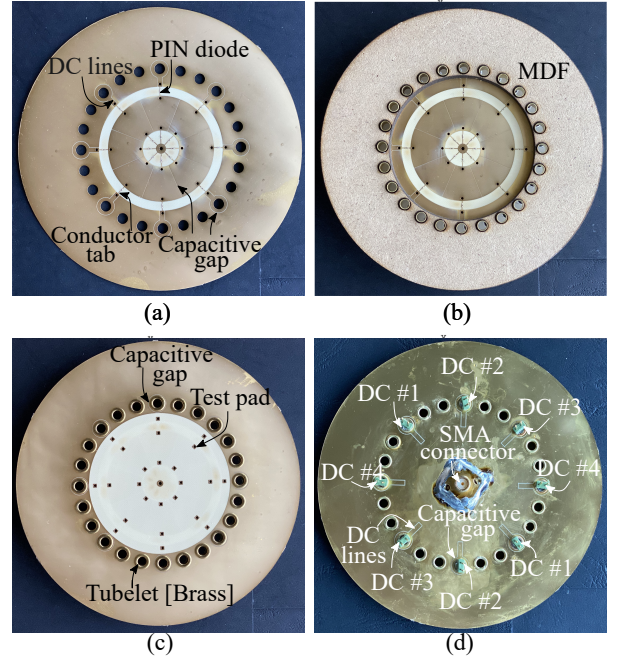


Fig. 4. Fabricated AFSIW cavity-backed slot antenna with multipolarization-reconfiguration. (a) Back side of Layer A. (b) Integrated Layer A inside Layer B. (c) Top view of assembled prototype. (d) Back side of Layer C.

mechanisms, including diode loss (on average 1%), conductor loss (on average 2%), and substrate loss (on average 1.5% for Layer B and 2.5% for Layer A), were also quantified. The result is shown in Fig. 3.

B. DC Power Consumption versus Antenna Efficiency

In the proposed design, only four PIN diodes are biased in the ON state in each polarization state, while the others are switched OFF, so only approximately a quarter of them are dissipating power. Moreover, by biasing the PIN diodes with the minimum bias current (1 mA) to polarize them in their forward state, the DC power consumption can be reduced. Yet, reducing the DC bias current to its minimum will increase the RF series resistance since the active PIN diodes act as current-controlled RF resistors. Hence, an inherent trade-off between DC power consumption and the total antenna efficiency arises. The optimal DC bias current in terms of DC power consumption and antenna radiation efficiency is found by evaluating the measured total antenna efficiency for different bias current values [see Section IV].

IV. MEASUREMENT RESULTS

Fig. 4 presents the fabricated prototype of the AFSIW cavity-backed slot antenna with multipolarization reconfiguration. The performance of the antenna is analyzed in an anechoic chamber, using a Keysight N5242a PNA-X network analyzer and an NSI-MI spherical near-field scanner. A Keithley 2450 source meter and an SHF Communication Technologies, SHF BT45A bias tee were employed for DC biasing.

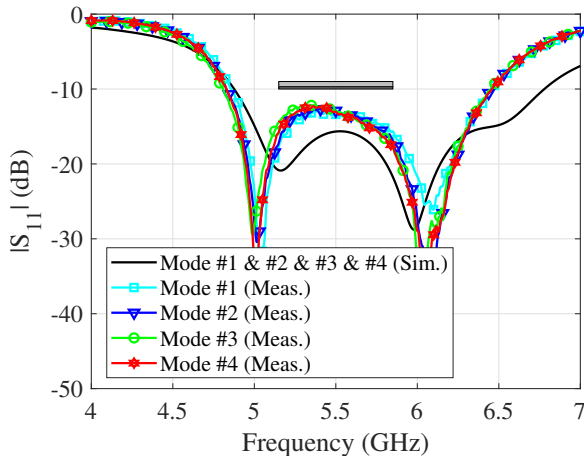


Fig. 5. Measured and simulated $|S_{11}|$ w.r.t. 50Ω for four modes.

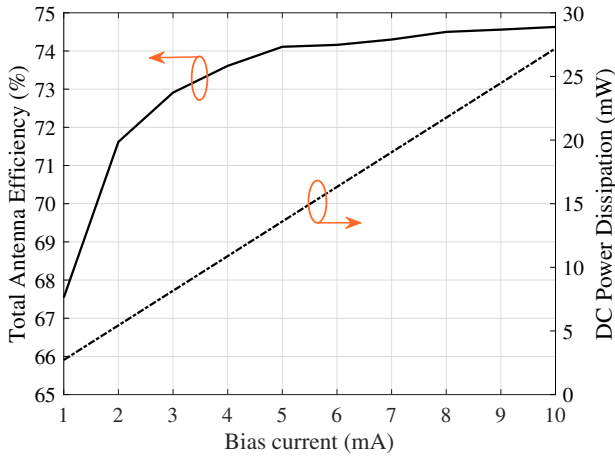


Fig. 6. Measured total antenna efficiency at 5.5 GHz and DC power dissipation as a function of DC bias current.

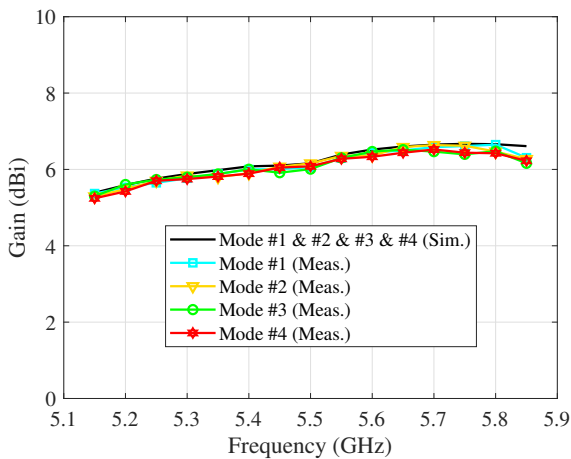


Fig. 7. Measured and simulated gain versus frequency for four modes.

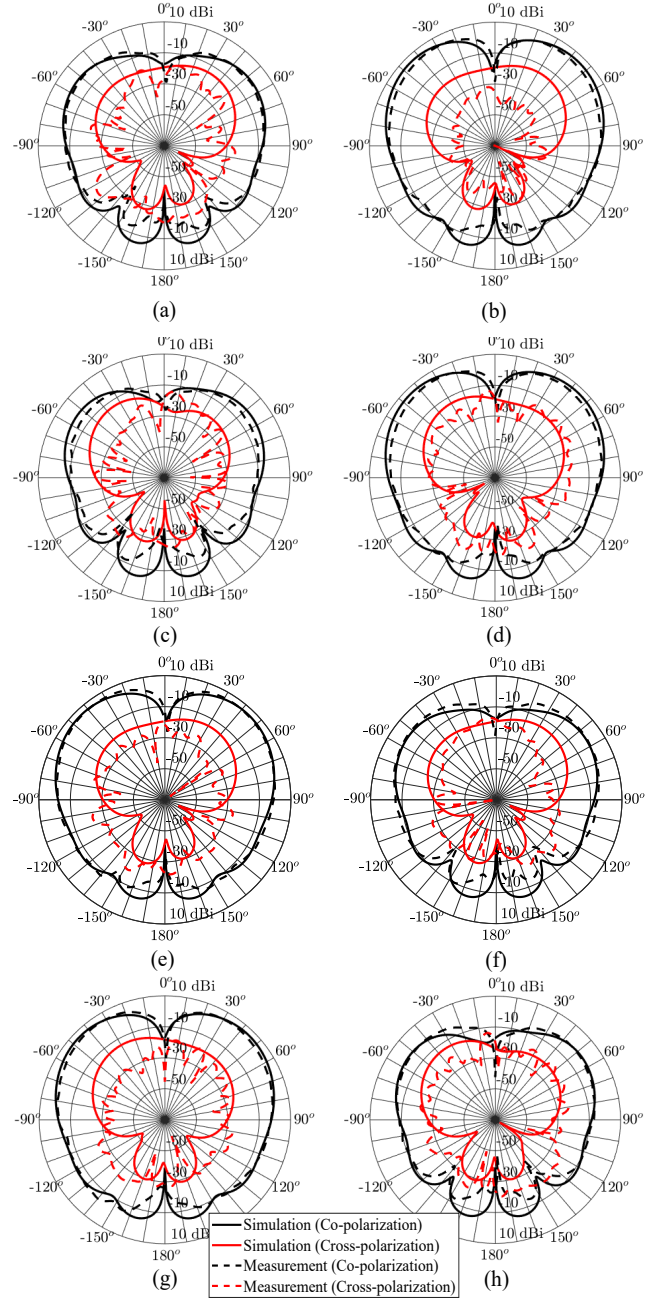


Fig. 8. Measured and simulated radiation patterns at 5.5 GHz. Mode#1: (a) $\phi = -45^\circ$ -plane and (b) $\phi = 45^\circ$ -plane. Mode#2: (c) $\phi = 0^\circ$ -plane and (d) $\phi = 90^\circ$ -plane. Mode#3: (e) $\phi = -45^\circ$ -plane and (f) $\phi = 45^\circ$ -plane. Mode#4: (g) $\phi = 0^\circ$ -plane and (h) $\phi = 90^\circ$ -plane.

Fig. 5, depicting the magnitude of the input reflection coefficient $|S_{11}|$ in four operating states with respect to $Z_0 = 50 \Omega$, depicts a good agreement between the measurement results of the fabricated prototype and simulation. A -10 dB impedance bandwidth of 1.6 GHz is obtained around the 5.5 GHz unlicensed national information infrastructure (U-NII) radio bands.

Fig. 6 illustrates the effect of the different DC bias currents on the measured DC power dissipation and total antenna

efficiency. As seen in Fig. 6, the DC power dissipation is only 27 mW when the DC bias current is set to 10 mA. In addition, it can be further reduced to 2.8 mW by biasing the PIN diodes with a reduced bias current of 1 mA. However, by reducing the bias current from 10 mA to 1 mA, the total antenna efficiency reduces significantly from 74.5% to 67%. In fact, this reduction can be attributed to a higher mismatch and lower radiation efficiency due to the higher PIN diode RF resistance at lower bias currents.

The simulated and measured realized gain of four linear polarization states across the operating band is depicted in Fig. 7. The antenna yields a stable gain of 5.2 dBi for the four polarization states.

Fig. 8 shows a good agreement between the simulated and measured gain pattern in the $\phi = -45^\circ$, $\phi = 0^\circ$, $\phi = 45^\circ$, and $\phi = 90^\circ$ planes at 5.5 GHz. A measured maximum gain of 5.8 dBi along the direction $(\theta, \phi) = (44^\circ, -45^\circ)$, a 3-dB beamwidth of higher than 45° and total efficiency of 74.5% is obtained at 5.5 GHz for a bias current of +10 mA, meaning that the antenna exhibits 45° -oriented linear polarization. Moreover, a front-to-back ratio larger than 10.5 dB is measured, while remaining the cross-polarization ratio within the 3-dB beamwidth higher than 20 dB. It is found that the radiation performances of four polarization states are identical, owing to the symmetry in the antenna topology.

V. CONCLUSION

We have presented full characterization of an AFSIW cavity-backed slot antenna exhibiting a wide bandwidth and featuring dynamic polarization reconfiguration. The proposed topology, whose concept was demonstrated here by incorporating four quartets of PIN diodes to support four linear polarizations, is versatile in terms of the number of available polarization states and orientation of the polarization. Moreover, it was shown that the proposed topology allows preserving high radiation efficiency and low cross polarization for a reconfigurable antenna.

VI. ACKNOWLEDGMENT

The authors would like to thank the ERC for the advanced grant 695495 "ATTO: A new concept for ultra-high capacity wireless networks".

REFERENCES

- [1] K. Rose, S. Eldridge, and L. Chapin, "The Internet of Things: An overview understanding the issues and challenges of a more connected world," *The Internet Soc.*, vol. 80, pp. 1-50, Oct. 2015.
- [2] H. Sundmaeker, P. Guillemin, P. Friess, and S. Woelfflé, "Vision and challenges for realising the Internet of Things," Eur. Commission Cluster Eur. Res. Projects Internet Things, vol. 3, no. 3, pp. 34-36, 2010.
- [3] Y. J. Guo, P.-Y. Qin, S.-L. Chen, W. Lin, and R. W. Ziolkowski, "Advances in reconfigurable antenna systems facilitated by innovative technologies," *IEEE Access*, vol. 6, pp. 5780-5794, Jan. 2018.
- [4] C.G. Christodoulou, Y. Tawk, S.A. Lane, and S.R. Erwin, "Reconfigurable antennas for wireless and space applications," *Proc. of the IEEE*, vol. 100, no. 7, pp. 2250-2261, July 2012.
- [5] H. Wong, W. Lin, L. Huitema, and E. Arnaud, "Multi-polarization reconfigurable antenna for wireless biomedical system," *IEEE Trans. Biomed. Circuits and Systems*, vol. 11, no. 3, pp. 652-660, June 2017.
- [6] H.H. Tran, N. Nguyen-Trong, T.T. Le, A.M. Abbosh, and H.C. Park, "Low-profile wideband high-gain reconfigurable antenna with quad-polarization diversity," *IEEE Trans. Antennas Propag.*, vol. 66, no. 7, pp. 3741-3746, July 2018.
- [7] W. Lin and H. Wong, "Multipolarization-reconfigurable circular patch antenna with L-shaped probes," *IEEE Antennas Wireless Propag. Lett.*, vol. 16, pp. 1549-1552, 2017.
- [8] W.-J. Sun, W.-W. Yang, L. Guo, W. Qin, and J.-X. Chen, "A circularly polarized dielectric resonator antenna and its reconfigurable design," *IEEE Antennas Wireless Propag. Lett.*, vol. 19, no. 7, pp. 1088-1092, Jul. 2020.
- [9] D. Chen, Y. Liu, S.-L. Chen, P.-Y. Qin, and Y.J. Guo, "A wideband high-gain multilinear polarization reconfigurable antenna," *IEEE Trans. Antennas Propag.*, vol. 69, no. 7, pp. 4136-4141, July 2021.
- [10] F. Wu, and K. M. Luk, "Wideband tri-polarization reconfigurable magneto-electric dipole antenna," *IEEE Antennas Wireless Propag. Lett.*, vol. 65, no. 4, pp. 1633-1641, Apr. 2017.
- [11] L. Song, W. Gao, and Y. Rahmat-Samii, "3-D printed microfluidics channelizing liquid metal for multipolarization reconfigurable extended E-shaped patch antenna," *IEEE Trans. Antennas Propag.*, vol. 68, no. 10, pp. 6867-6878, Oct. 2020.
- [12] S.-L. Chen, F. Wei, P.-Y. Qin, Y. J. Guo, and X. Chen, "A multi-linear polarization reconfigurable unidirectional patch antenna," *IEEE Trans. Antennas Propag.*, vol. 65, no. 8, pp. 4299-4304, Aug. 2017.
- [13] L. Ge, Y. Li, J. Wang, and C.-Y.-D. Sim, "A low-profile reconfigurable cavity-backed slot antenna with frequency, polarization, and radiation pattern agility," *IEEE Trans. Antennas Propag.*, vol. 65, no. 5, pp. 2182-2189, May 2017.
- [14] N. Nguyen-Trong, A. Piotrowski, L. Hall, and C. Fumeaux, "A frequency and polarization-reconfigurable circular cavity antenna," *IEEE Antennas Wireless Propag. Lett.*, vol. 16, pp. 999-1002, 2017.
- [15] L.-H. Chang, W.-C. Lai, J.-C. Cheng, and C.-W. Hsue, "A symmetrical reconfigurable multipolarization circular patch antenna," *IEEE Antennas Wireless Propag. Lett.*, vol. 13, pp. 84-90, 2014.
- [16] K.Y. Kapsuz, S. Lemey, P. Demeester, and H. Rogier, "Ultra-wideband and substrate-independent AFSIW cavity-backed slot antenna for high-performance smart surfaces," in *Eur. Microw. Conf.*, London, UK, 2022.
- [17] K.Y. Kapsuz, S. Lemey, A. Petrocchi, P. Demeester, D. Schreurs, and H. Rogier, "Polarization reconfigurable air-filled substrate integrated waveguide cavity-backed slot antenna," *IEEE Access*, vol. 7, pp. 102628-102643, 2019.
- [18] K.Y. Kapsuz, S. Lemey, and H. Rogier, "Multipolarization reconfigurable air-filled substrate integrated waveguide cavity-backed slot antenna," *IEEE Antennas and Wireless Propag. Lett.*, vol. 20, no. 4, pp. 622-626, April 2021.
- [19] K.Y. Kapsuz, S. Lemey, and H. Rogier, "Substrate-independent microwave components in substrate integrated waveguide technology for high-performance smart surfaces," *IEEE Trans. Microw. Theory Techn.*, vol. 66, no. 6, pp. 3036-3047, June 2018.
- [20] K.Y. Kapsuz, S. Lemey, P. Demeester, and H. Rogier, "Additive-manufacturing-enabled air-filled substrate integrated waveguide microwave components," in *IEEE Int. Symp. on Antennas and Prop. & USNC/URSI Nat. Radio Sci. Meeting*, Boston, MA, USA, 2018, pp. 939-940.
- [21] M. Bozzi, M. Pasian, L. Perreggini, and K. Wu, "On the losses in substrate-integrated waveguides and cavities," *International Journal of Microw. and Wireless Technologies*, vol. 1, no. 5, pp. 395-401, October 2009.
- [22] A. Ghiotto, F. Parment, T. Martin, T.P. Vuong, and K. Wu, "Air-filled substrate integrated waveguide - A flexible and low loss technological platform," in *Int. Conf. on Adv. Technol., Syst. and Services in Telecommun.*, Nis, Serbia, 2017, pp. 147-149.